



## Structure and Variability of Indonesian Throughflow in Libani Canal

Rizqi Rizaldi Hidayat<sup>1\*</sup>, Mukti Trenggono<sup>1</sup>

<sup>1</sup> Department of Marine Science, Fishery and Marine Science Faculty, Jenderal Soedirman University, Purwokerto 53122 INDONESIA

\*Corresponding author: [rizaldi.rizqi@gmail.com](mailto:rizaldi.rizqi@gmail.com)

Received 5 August 2018; Accepted 20 November 2019; Available online 26 November 2019

### ABSTRACT

Libani Canal is one of the areas which the flows water masses of the Pacific Ocean toward Indonesian seas. The existence of Mindanao current that affects an input of Indonesian Throughflow should be predicted. The influence of climate change on large scale circulation will affect the variations of physical condition. This study focused to investigate the variation of meridional Libani Current at 30 levels deep based on INDESO models data from January 2007 to January 2014. An area of interested was located at 4.16 °S and 117.92 - 119.42 °E. The results showed a strong current average reaches 0.5 m/s with a north-south orientation as the impact of bottom topography. Variations of current through Fourier analysis showed the annual and inter-annual fluctuations in the 365 days and 120-200 days related impacts strong El-Nino in 2009-2010. Spectrum energy density peaks in the 3 days and 53 days period that indicated as the impact of intra-seasonal variations.

**Keywords:** *variability, Indonesian Throughflow, Libani Canal, INDESO*

### ABSTRAK

Kanal Libani adalah salah satu daerah yang mengalirkan massa air Samudra Pasifik ke Perairan Indonesia. Keberadaan arus Mindanao yang memengaruhi input Arus Lintas Indonesia perlu diprediksi. Pengaruh perubahan iklim pada sirkulasi skala besar akan mempengaruhi variasi kondisi fisik. Penelitian ini berfokus untuk menyelidiki variasi arus Libani meridional pada kedalaman 30 level berdasarkan data model INDESO dari Januari 2007 hingga Januari 2014. Area yang diminati terletak pada 4,16 °S dan 117,92 - 119,42 °E. Hasil penelitian menunjukkan rata-rata arus yang kuat mencapai 0,5 m/s dengan orientasi utara-selatan sebagai dampak topografi bawah. Variasi saat ini melalui analisis Fourier menunjukkan fluktuasi tahunan dan antar-tahunan dalam 365 hari dan 120-200 hari terkait dampak kuat El-Nino pada 2009-2010. Puncak kepadatan energi spektrum dalam periode 3 hari dan 53 hari yang ditunjukkan sebagai dampak dari variasi intra-musiman.

**Kata Kunci:** *variabilitas, Arlindo, Kanal Libani, INDESO*

### 1. Introduction

The flow of water from Pacific to the Indian Ocean through Indonesia archipelago or us we call The Indonesian Throughflow (ITF) or in Bahasa Indonesia, *Arus Lintas Indonesia* (Arlindo) is a famous and interesting topic among the oceanographers

and the general public in recent years. ITF from the Pacific Ocean entrances to the Indian Ocean that passed through the Indonesian sea via two paths, the west and east path where the components of the water mass composed the mass of the North Pacific and South Pacific water (Wyrcki, 1961; Gordon and Fine, 1996). The west path of the

ITF route is the mass of water from the Pacific Ocean carried by the Flow of Mindanao entering through the Sulawesi Sea into the Makassar Strait then in the Flores Sea, part of the mass of water going out into the Indian Ocean through the Lombok strait and the rest going to the Banda Sea. The second path is eastern path, the mass of water from the Pacific Ocean through the Maluku Sea and the Halmahera Sea to the Seram Sea then proceed to the Banda Sea. In the Banda Sea there was a meeting of water masses from the west and east lines and then out to the Indian Ocean through the Ombai Strait and Timor passage (Fieux et al., 1996; Atmadipoera et al., 2009).

Makassar strait as the main entrance of the ITF now carries the ITF transport about 75% of 15 Sv ( $Sv = 10^6 \text{ m}^3\text{s}^{-1}$ ) total transport that carries water masses from the North Pacific Ocean (Gordon et al., 2010; Susanto et al., 2012, Li et al., 2018). The ITF water mass from the North Pacific consists of a mass of North Pacific Subtropical Water (NPSW) in the thermocline layer and North Pacific Intermediate Water (NPIW) in the lower thermocline layer. NPSW and NPIW entering Indonesian Seas have characteristics of high (maximum) salinity values for NPSW and low (minimum) salinity values for NPIW. In the Makassar Strait, found that below the surface potential density of  $24.25 \sigma_\theta$  stratifications of water masses are dominated by Makassar ITF with salty (34.6 psu) North Pacific thermocline water (NPSW) and less salty (34.42 psu) North Pacific lower-thermocline water (NPIW) (Prihatiningsih et al., 2019). The canal contour of the strait affects the character of the moving water mass.

ITF has high variability both seasonally and annually. Seasonal variability is influenced by the change of wind or monsoon direction in Indonesia, which is then called Indonesian Monsoon Flow (Armondo) which is found in the surface layer with a depth of 0-50 meters (Ilahude, 1996). The strongest flow of Arlindo water mass occurs during the southeast monsoon from June to August, while the lowest flow occurs during the northwest monsoon, December to February (Wyrski, 1987). Arlindo's annual variability is related to the occurrence of the El Niño Southern Oscillation (ENSO) phenomenon, which affects the global climate globally.

One method that can be used in describing the variability found in Libani Canal is by using time series analysis. This method aims to determine the variability of a periodic data series and determine the periodicity of the observed data variables (Thomson and Emery, 2014). The basic concept of time series analysis method is observing data based on time and space, the results can explain changes that occur in time and changes in space (Thomson et al., 2014). The time-series analysis used in processing oceanography signals helps us to describe the characteristics of the variables that exist in the ocean in accordance with the time series of events so that patterns are expected to be a characteristic of these waters.

## 2. Materials and Methods

### 2.1. INDES0 model data

The simulation results of the marine general circulation model with the INDES0 (Infrastructure Development of Space Oceanography) configuration from 2007-2014 were used in this paper. Compared to similar ocean modeling systems in the Indonesian region (eg HYCOM, OFES), the INDES0 model has several advantages, such as explicitly applied baroclinic and barotropic tidal forcing, atmospheric forcing with high temporal and spatial resolution, seafloor topography regulation in narrow strait region, as well as intensive validation of the simulation results of water currents and masses with field data with satisfactory results (Tranchant et al., 2015). The INDES0 model uses the NEMO modeling system (Madec, 2008). In complete configuration and validation the INDES0 model is explained in Tranchant et al. (2015). A brief description of this model configuration has a horizontal resolution of  $1/12^\circ$  or about 9.25 km with 50 vertical levels where the vertical resolution near the surface is denser (about 1 m), and increasingly tenuous with increasing depth. Bathymetry data are based on ETOPO2 Version 2' and GEBCO Version 1' data. The high temporal resolution (3-hour) atmospheric drive was obtained from data from the European Center for Medium Range Weather Forecasts (ECMWF). The barotropic tidal drive at open limits for the 10 main tidal components is obtained from

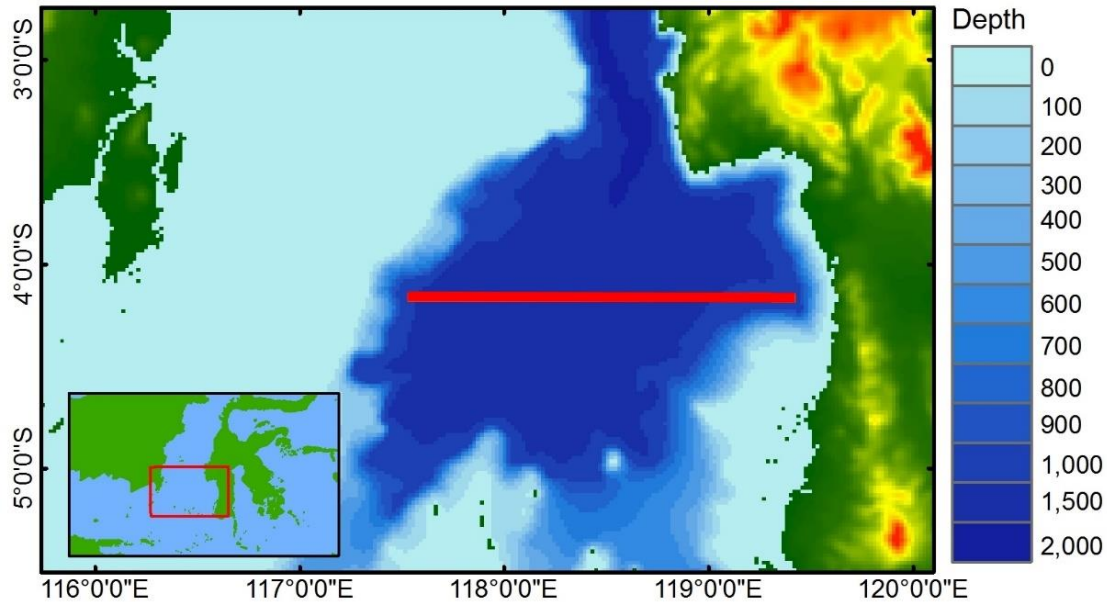


Figure 1. Map of study locations overlaid with bathymetry data; red line is an observation transect

TPX07. Tidal drives are applied explicitly or implicitly (parameterization), so that the physical process of mixing can be accurately modeled (Figure 1).

The INDES0 model is one of the marine programs of the Ministry of Maritime Affairs and Fisheries, which is supported by 2 Europa marine research institutes (Mercator-Ocean and Collecte Localisation Satellites - CLS) for the development of oceanography operational in Indonesia. The control center for INDES0's oceanographic operational program is centered at the Bali Ocean Observation and Modeling Center (BPOL). The output of the INDES0 model used in this study, in the form of 3-dimensional zonal and meridional current component variables with daily averages from 2007 to 2014.

## 2.2. Data Analysis

Fourier series is a method developed from a function called periodic function. A function can be periodic if the function satisfies the relationship  $f(x) = f(x + L)$ , with  $L$  being the period of the function. Fourier series was first developed by Joseph Fourier (1768-1830). In Fourier series, a periodic function is described as the number of sine and cosine's functions that can be expressed in the equation:

$$y(t) = \overline{y(t)} + \sum_p [A_p \cos(\omega_p t) + B_p \sin(\omega_p t)]$$

where is the data value, and is a constant (Fourier coefficient), and the value of is the value of the angular frequency (Thomson and Emery, 2014).

Fourier transform is a transformation model that moves the spatial domain or time domain into the frequency domain. Fourier transformation that is done manually encounters obstacles, namely the time needed (especially in computing) to transform data takes a long time. To overcome this problem, a method is known as Fast Fourier Transform is introduced. Fast Fourier transform (FFT) is an efficient algorithm for calculating discrete Fourier transform (DFT) and its inverse (Parker, 2017) Fast Fourier transform (FFT) becomes important for various applications, from processing digital signals and solving partial differential equations to algorithms for doubling a large number of integers.

The wavelet function complements the limitations of Fourier analysis, which can detect sine and cosine waves in nonstationary data. The superiority of wavelet is that it is able to analyze locally (short time but with greater signal). Wavelet is divided into 2, namely Cross Wavelet Transform (CWT) and Discrete Wavelet Transform (DWT). In this case, we use CWT to analyze data. The workings of CWT are the sum of the entire time of the signal  $f(t)$  multiplied by the shifted and scaled version of

the wavelet function to produce a wavelet coefficient. In this CWT the terms *scaling* and *shifting* are used, where *scaling* is the stretching of the wavelet function while *shifting* is shifting with the same signal so that it can speed up or slow down the wavelet function.

Correlation is a method used to find the closeness of relationships between data variables and the variables themselves. Correlation itself consists of autocorrelation (a time series variable that is correlated to the variable itself) and cross-correlation (a time series data variable that is correlated to other variables). The working principle of this correlation is by shifting the time series data in some shifts.

### 3. Result and Discussion

#### 3.1. Temporal Fluctuation of Temperature, SSH, Current and Wind

The time-series graph of the average temperature of the Libani Canal (Figure 2) at high frequency and low-frequency show daily

and annual fluctuations. The lowest average surface temperature occurs between July-August, and the highest average temperature occurs around February. This is due to seasonal changes due to the monsoon system that occurs above the waters of the Libani Strait. Temperature values in the Libani Canal range between 16.8-19 °C. The minimum and maximum temperature values are not right at the peak of each rainy and dry season. This is caused by a time lag or a time lag for the value of the temperature change. Fluctuations in the average temperature that occurs in Libani waters range from  $\pm 1.2$  °C to -1 °C.

The sea level height variable (SSH) shown in Figure 3 shows that the highest value of the water level reaches 0.85 m and the lowest is 0.55 m. The SSH plot pattern, in general, is almost the same as the average temperature pattern. The values of visible fluctuations range from -0.14 m to +0.17 m. The highest average values are seen at the beginning of the year or around February to March. This is happen because the influence of the West or the rainy season. Similar to

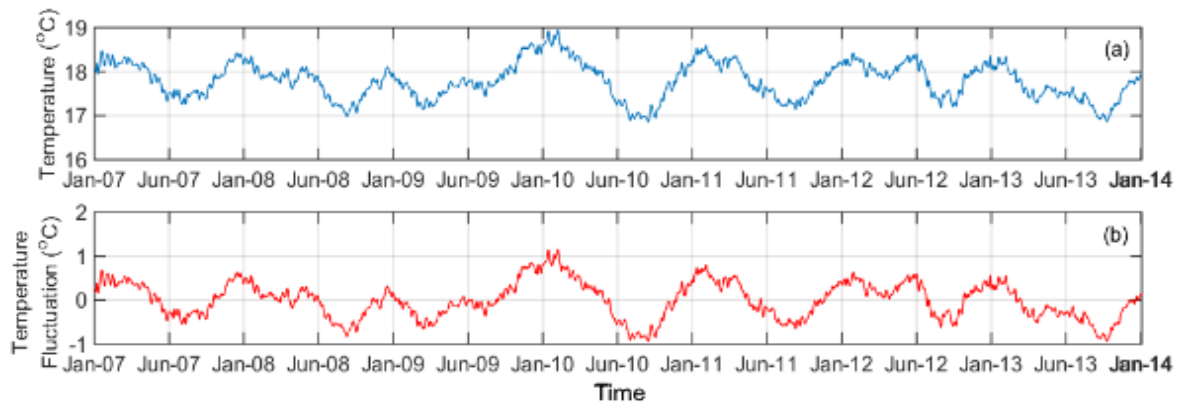


Figure 2. Time series data of (a) temperature and (b) temperature fluctuation in Libani Canal

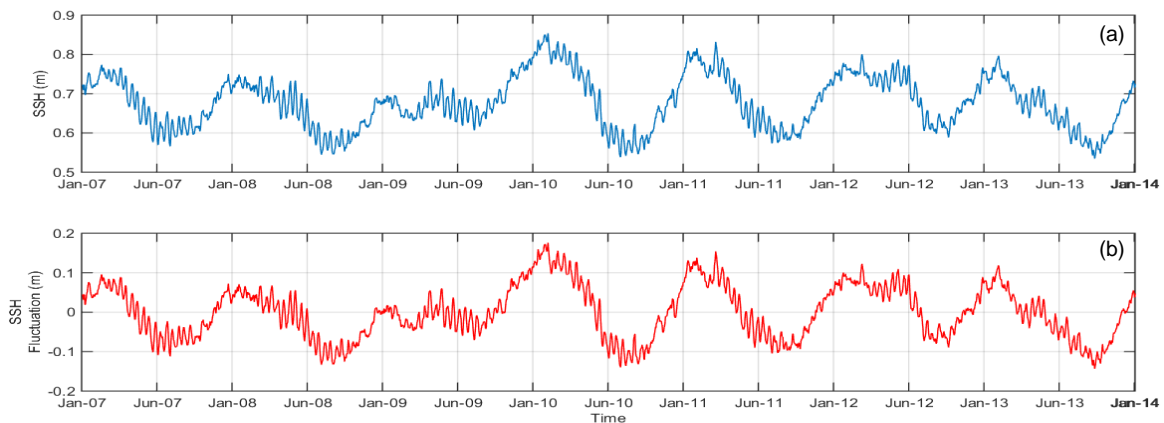


Figure 2. Time series data of (a) SSH and (b) SSH fluctuation in Libani Canal

temperature patterns, sea-level rise and lowest values are not suitable in the rainy and dry seasons.

The dominant current that occurs in the Libani Canal is the meridional current (Figure 4), which is the current that flows from north to south or vice versa. The average value shows that the direction of flow in these waters is very volatile because in these waters influenced by Armondo and Arlindo. Surface currents in the Libani Canal show strong seasonal variations, where in the western monsoon there are low salinity surface flows (currents) originating from the South China Sea (Gordon et al., 2003). According to Sprintall et al., (2014) Arlindo's depth and speed variations are also influenced by the presence of El Niño Southern Oscillation (ENSO) and Indian Ocean Dipole (IOD) in periods of time between years or decades. During 2004-2009 El Niño occurred with a positive IOD in 2006/ 2007 and La Niña with a neutral IOD during the 2007/2008 period (Susanto et al., 2012).

El Niño causes the Pacific trade winds to weaken or reverse so that Arlindo's

transportation is weak (Sprintall et al., 2014). Entering the Libani Canal, the Arlindo flow has intensified. The narrow and deep Libyan Canal configuration (2000 m) is a major factor in the strong flow of the region. In the Libani Canal, branching has begun to occur to the west and east side of the strait. Gordon and Fine (1996) suggest that the branch of the Arlindo flow occurs when the Arlindo current passes through Dewakang Sill (680 m). However, according to Horhoruw et al., (2015), branching now occurs before crossing the Dewakang threshold. Before entering the Libani Canal area, the depth of the water contour was around 2000 m, then further south where branching is currently found to reduce bathymetry by more than 300 meters with a peak contour of 1771 m. The direction of the dominant average is South with speeds ranging from 0.3 - 0.12 m/s. Flow fluctuations from -0.03 to +0.05 m/s (Figure 5).

Libani waters are affected by monsoons which consist of monsoons and monsoons. However, due to its location sandwiched between 2 islands, the dominant wind direction is meridional or north-south.

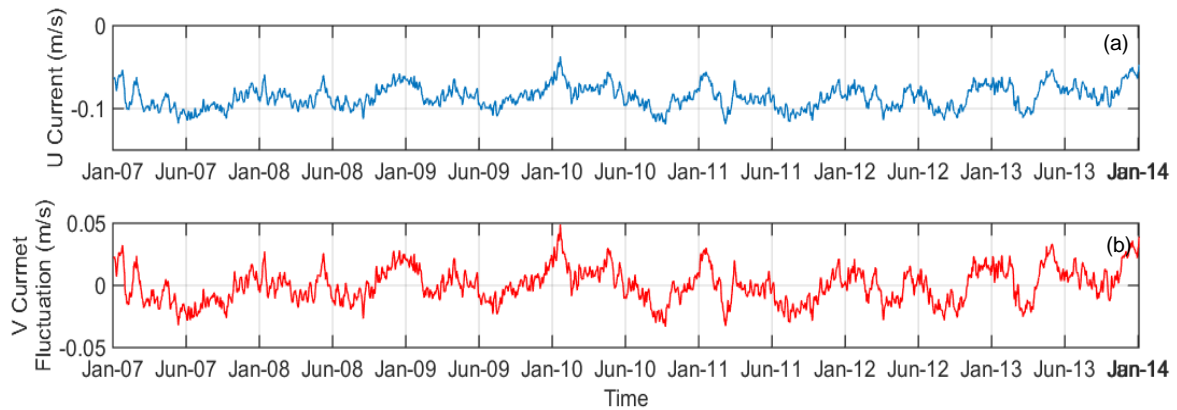


Figure 4. Time series data of (a) current and (b) current fluctuation in Libani Canal

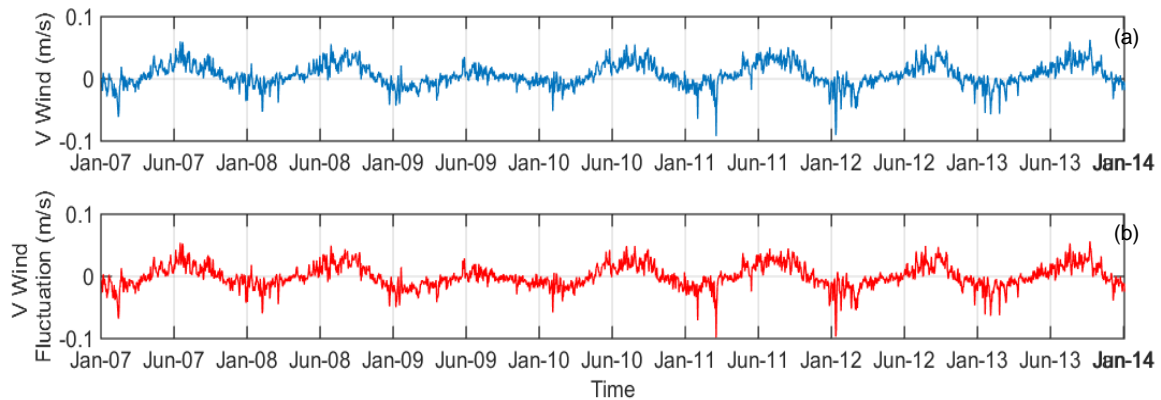


Figure 5. Time series data of (a) wind and (b) wind fluctuation in Libani Canal

The wind speed that occurs in the Libani Canal is not much different from the current speed (Figure 5). The wind speed fluctuates at half-yearly or season which is almost the same as the monsoon pattern, which changes direction twice a year, namely the west monsoon and east monsoon. Meridional wind fluctuation graphs show that the positive value of the wind flows from south to north, and the negative value indicates that the wind flows to the south.

### 3.2. Variability of Temperature, SSH, Current, and Wind

To find out temporal fluctuations of temperature, SSH, current and wind, the Fast Fourier Transform (FFT) method is presented in Figures 6. The figure provides information based on frequency, each variable responds to the highest amplitude value in the frequency range between 0.01 cpd to 0.001 cpd. The amplitude value in the graph illustrates the strength of each variable's anomaly for a certain frequency range.

In the temperature variable, the highest amplitude appears at intervals of  $1 \times 10^{-3}$  cpd to  $2 \times 10^{-3}$  cpd, precisely in periods 365 days to 852 days (Figure 6a). This shows that the surface temperature of Libani Canal has two dominant periods,

namely the seasonal period and the annual period. The average temperature period in the Libani waters, which is the annual period, can be influenced by several factors, such as monsoonal changes and exist Arlindo crossing these waters. Moreover, it can be caused by the area of Libani waters being influenced by input from the land (Kalimantan and Sulawesi Islands) and due to monsoonal changes. Input from the land originating from rivers flowing on the Kalimantan island's land body contributes to seasonal fluctuations in temperature. This is closely related to the amount of rain which then enters the river and flows into the waters of the Makassar Strait, which is likely to decrease the surface temperature of the waters in the Libani Waters. In addition, the monsoon winds that change periodically every midyear become one of the factors that cause the change in the surface temperature of Libani waters to be semi-annual. The other periods are not too dominant but still have an influence on temperature fluctuations that occur in the observation area.

The SSH variable gives a response that is not much different from the temperature variable, where the period with the highest amplitude value is achieved in the 365 day period (Figure 6b). This shows that

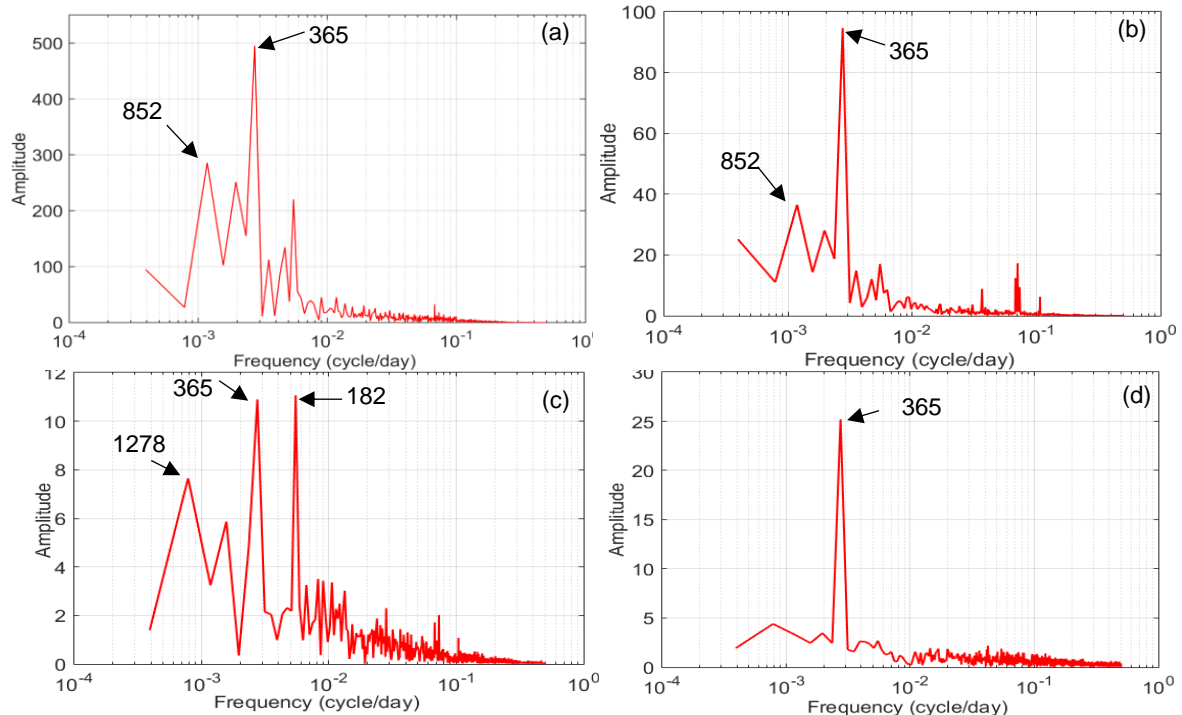


Figure 6. FFT graphs of (a) temperature, (b) SSH, (c) current, and (d) wind in Libani Canal, numbers on the arrows indicate periods in days

the water level in the Libani waters changes with seasonal patterns. If the western season, the value of sea level increases, and vice versa if the east season sea level is decreased, or decreases. The dominant period pattern in the current measure is annual (annual), likewise, the wind has an annual dominant period (annual).

The graph in Figure 7 shows the different response periods between observation variables in the observation area using the Continue Wavelet Transform (CWT) method. The variable temperature CWT chart at Libani Canal gives or shows a very strong response to temperature change fluctuations in 2010-2011 which reached the maximum value in that period. This response takes place in a period of between 300-400 days or referred to as annual fluctuation (Figure 7a).

The water surface height (SSH) in Libani Canal changes periodically every year with an annual periodicity. The maximum value (red) indicated the period 300-400 in 2010-2012 (Figure 7b). In addition, there is also a 10-day period of up to 16 days (inter-seasonal). Changes in water level (SSH) in the Libani Canal area are largely influenced by move water masses both from move ITF and wind friction on the surface (Nurjaya and Surbakti, 2009). Water levels in the Pacific

Ocean and the Indian Ocean will affect changes or fluctuations in water levels in the Libani Canal.

The current velocity on the Libani Canal shows annual fluctuations with a peak in 2009-2012. In 2013 there was a period of 120-200 days or so-called half-yearly (Figure 7c). This is caused by the existing 2 seasons in Indonesia that affect surface current circulation. In addition, there are also high periods at 20-30 days (intra-seasonal) and 3-25 days. The complexity of the variable periodicity due to currents in these waters is influenced by monsoons and the presence of Arlindo. The wind speed in the Libani Canal experiences annual fluctuations because in Indonesia there are 2 seasons, the West and East Seasons.

Figure 8 is a graph of the results of the cross-correlation between surface temperature and the meridional current in the surface layer of the Libani Canal. The results of the cross-correlation show negative values, this shows that changes in the current variables do not affect changes in temperature in the Libani Canal. The auto-correlation values for the Meridional Flow variable show symmetry between the correlation values in the time before the maximum correlation phase and after the maximum correlation phase. The correlation

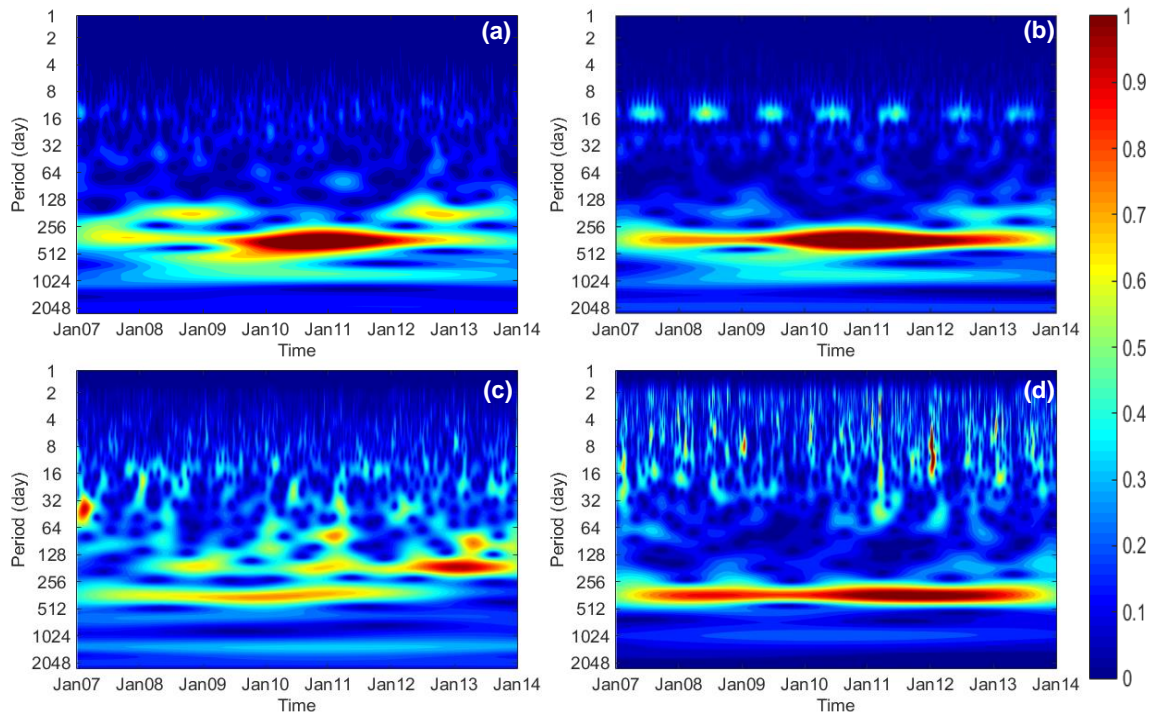


Figure 7. Graphs of continuous wavelet transformations for (a) time series temperature, (b) time series SSH, (c) time series current and (d) time series wind in Libani Canal

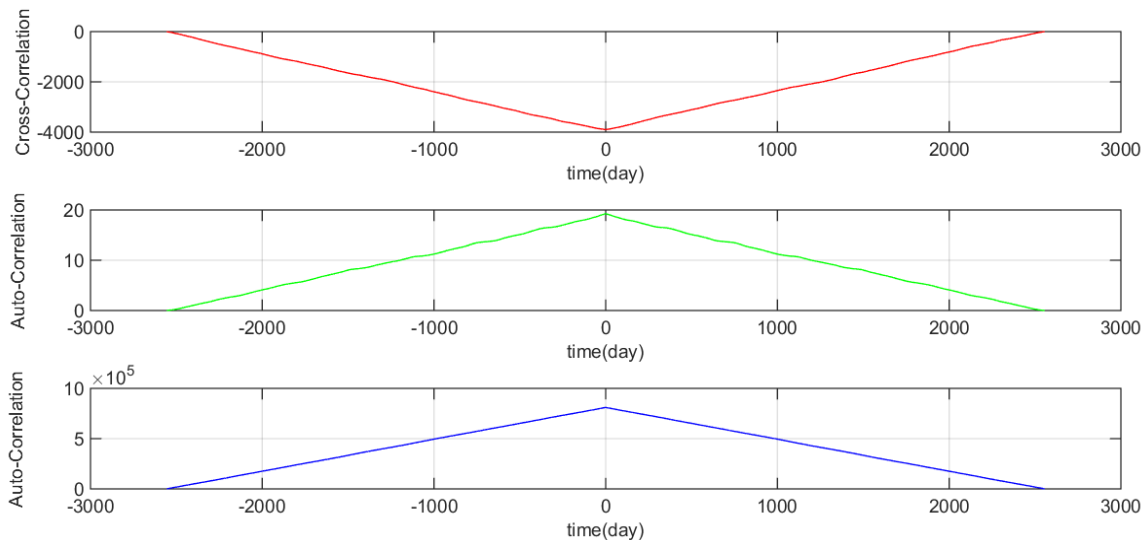


Figure 8. Cross Correlation and Auto Correlation

coefficient given is 1 so that changes in sea surface temperature have a definite periodicity pattern. Changes in current that occur will greatly affect changes in flow at a later time. Like meridional flow, the autocorrelation value in the meridional wind variable also shows a value of 1, so it can be concluded that changes in the wind at present can affect changes in the wind in the future.

#### 4. Conclusion

Libani Canal is one of the areas which the flows water masses of Pacific Ocean to Indian Ocean toward Indonesian seas. Arlindo's annual cycle on the Libani Canal is characterized by the magnitude of the flow rate and width of the Arlindo Makassar Jet which is stronger in the East Season compared to the West Season. The variability of flows in inflow locations fluctuates at the dominant seasonal scale periodicity (180 daily) with energy peaks in the periodicity between daily and annual.

#### References

- Atmadipoera A.S., Molcard, R., Madec, G., Wijffels, S., Koch-Larrouy, A., Jaya, I., Supangat, A., Sprintall, J. 2009. Characteristics and variability of the Indonesian throughflow water at the outflow straits. *Deep-Sea Research I* 56, 1942-1954.
- Fioux, M., Andrie, C., Charriaud, E., Ilahude, A.G., Metzl, N., Molcard, R., Swallow, J.C. 1996. Hydrological and chlorofluoromethane measurements of the Indonesian throughflow entering the Indian Ocean. *Journal of Geophysical Research* 101, 12433-12454.
- Gordon A.L. and R.A. Fine. 1996. Pathways of water between the Pacific and Indian Ocean in the Indonesian Sea. *Nature*. 379: 146-149
- Gordon, A.L., Susanto, R.D., Vranes, K. 2003. Cool Indonesian throughflow as a consequence of restricted surface layer flow. *Nature* 425, 824-828.
- Gordon, A., Sprintall, J., Van Aken, H.M., Susanto, R.D., Molcard, R., Ffield, A., Pranowo, W., Wirasantosa, S., Wijffels, S. 2010. The Indonesian throughflow during 2004-2006 as observed by the INSTANT program. *Dynamics of Atmospheres and Oceans* 50(2), 115-128.
- Horhoruw, S.M., Atmadipoera, A.S., Purba, M., Purwandana, A. 2015. Struktur arus dan variasi spasial Arlindo di Selat Makassar dari EWIN 2013. *Ilmu Kelautan* 20(2), 87-100.
- Ilahude A.G., Gordon, A.L. 1996. Thermocline stratification within the Indonesian Seas. *Journal of*



- Geophysical Research Atmospheres 101, 12401-12409.
- Li, M., Gordon, A.L., Wei, J., Gruenbug, L.K., Jiang, G. 2018. Multi-decadal timeseries of the Indonesian throughflow. *Dynamics of Atmospheres and Oceans* 81, 84-95.
- Madec, G., Delecluse, P., Imbard, M., and Lévy, C. 1998. OPA 8.1 Ocean General Circulation Model reference manual. Note du Pole de modélisation. Institut Pierre-Simon Laplace (IPSL). France. 91pp.
- Nurjaya, I.W. & Surbakti, H. 2009. Studi Pendahuluan Kondisi Oseanografi Fisik pada Musim Barat di Perairan Pantai Timur Kalimantan antara Balikpapan dan Delta Mahakam. *Jurnal Kelautan Nasional* 1, 140-150.
- Parker, M. 2017. Discrete and Fast Fourier Transforms. In: *Digital Signal Processing* 101 (Second Edition). Newnes Newton, MA, USA.
- Prihatiningsih, I., Jaya, I., Atmadipoera, A.S., Zuraida, R. 2019. Turbulent mixing of water masses in Selayar Slope - Southern Makassar Strait. *Proceedings of LISAT-FSEM 2018*. Bogor: 6-7 November 2018.
- Sprintall, J., Gordon, A.L., Koch-Larrouy, A., Lee, T., Potemra, J.T., Pujiana, K., Wijffels, S.E. 2014. The Indonesian seas and their role in the coupled ocean-climate system. *Nature Geoscience* 7:487-492.
- Susanto, R.D., Ffield, A., Gordon, A.L., Adi, T.R. 2012. Variability of Indonesian throughflow within Makassar Strait 2004-2009. *Journal of Geophysical Research Atmospheres* 117, 1-16.
- Thomson, R.E., Emery, W.J., 2014. *Data Analysis Methods in Physical Oceanography*. Elsevier, London. 728 pp.
- Tranchant, B., Reffray, G., Greiner, E., Nugroho, D., Saint-agne, R. 2015. Evaluation of an operational ocean model configuration at 1/12°spatial resolution for the Indonesian seas Part I. *Ocean physics*, 1-49.
- Wyrtki, K. 1961. *Scientific Results of Marine Invesigations of the South China Sea and the Gulf of Thailand 1959-1961*. Naga Report Volume 2.
- Wyrtki, K. 1987. Indonesian Through Flow and the Associated Pressure Gradient. *Journal of Geophysical Research Atmospheres* 92:12941-12946.